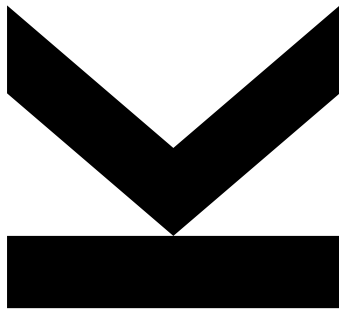


# **Semi-Supervised Anomaly Detection in Respiratory Sounds: A Comparative Study of Reconstruction and Density Estimation Methods**



Bachelor's Thesis

to confer the academic degree of

Bachelor of Science

in the Bachelor's Program

Artificial Intelligence

Author  
**Lukas Selch**  
11941656

Submission  
**Institute of  
Computational Perception**

Thesis Supervisor  
**Paul Primus**

December 2023

# Abstract

Space for your abstract.

# Contents

<b>Abstract</b>	<b>ii</b>
<b>1 Introduction</b>	<b>1</b>
1.1 Motivation . . . . .	1
1.2 Objectives and Approach . . . . .	1
1.3 Outline . . . . .	1
<b>2 Theoretical Background</b>	<b>2</b>
2.1 Respiratory Sounds . . . . .	2
2.1.1 Digital Representation of Sound . . . . .	2
2.2 Fundamentals of Anomaly Detection . . . . .	3
2.3 Reconstruction-Based Methods . . . . .	4
2.3.1 Essentials of Autoencoders . . . . .	5
2.4 Density Estimation Methods . . . . .	5
2.4.1 Introduction to Masked Autoencoders . . . . .	5
2.5 Evaluation Metrics for Model Comparison . . . . .	6
<b>3 Literature Review</b>	<b>9</b>
3.1 Current State of Respiratory Sound Analysis . . . . .	9
3.1.1 The ICBHI Challenge 2017 . . . . .	9
3.1.2 Existing Approaches . . . . .	10
3.2 Respiratory Sound Analysis from an Anomaly Detection Perspective	11
3.3 Variational Autoencoders . . . . .	11
3.4 Group Masked Autoencoders . . . . .	11
<b>4 Methodology</b>	<b>13</b>
4.1 Dataset . . . . .	13
4.1.1 Definition . . . . .	13
4.1.2 Data Splitting . . . . .	13
4.2 Preprocessing . . . . .	13
4.3 Detailed Overview of the Models . . . . .	13
4.3.1 Implementation of the VAE . . . . .	13
4.3.2 Implementation of the G-MADE . . . . .	13
<b>5 Experiments and Results</b>	<b>14</b>
5.1 Experimental Setup . . . . .	14
5.2 Generalization Capabilities . . . . .	14
5.3 Age and Gender Differences in Model Accuracy . . . . .	14
5.4 Model Sensitivity to Noise . . . . .	14
5.5 Model Performance on Crackles and Wheezes . . . . .	14
5.6 Impact of Hyperparameter Variations . . . . .	14
5.7 Assessment of Data Splitting at Recording Level . . . . .	14
5.8 Comparison of Feature Extraction Methods: MFCC vs. MelSpec- trogram . . . . .	14
5.9 Interpretability and Explainability of the Proposed Models . . . . .	14
5.10 Comparative Analysis and Discussion . . . . .	14
<b>6 Conclusion and Outlook</b>	<b>15</b>
6.1 Summary of Findings . . . . .	15

6.2	Potential Applications and Practical Implications . . . . .	15
6.3	Limitations of the Proposed Approaches . . . . .	15
6.4	Directions for Future Research . . . . .	15
	<b>Bibliography</b>	<b>16</b>

# Chapter 1

## Introduction

Respiratory diseases are a leading cause of premature mortality worldwide. With over four million annual deaths attributed to these diseases, early identification and treatment efforts are imperative [11]. The use of chest auscultation, a technique in which respiratory sounds are analyzed with instruments like stethoscopes, is a simple and effective way for diagnosing respiratory diseases.

Automated systems for detecting sound anomalies have become of increasing relevance in the medical field and are driving machine learning research [4]. They have the potential to improve diagnostic accuracy for healthcare professionals and provide initial assessments for patients, ultimately leading to more efficient allocation of healthcare resources.

### 1.1 Motivation

### 1.2 Objectives and Approach

### 1.3 Outline

# Chapter 2

## Theoretical Background

### 2.1 Respiratory Sounds

The respiratory system, which includes the airways and lungs, plays a crucial role in gas exchange, a vital function in the human body. Respiratory sounds, created by airflow during breathing, can reveal a lot about respiratory health [9]. These sounds, observed through a process called 'auscultation'—listening to the chest with a stethoscope—are critical for detecting respiratory diseases. This method is cost-effective, non-invasive, and a standard part of physical examinations [4].

We can categorize respiratory sounds into normal and anomalous based on their characteristics during auscultation. Normal sounds are typically heard during inhalation and at the start of exhalation, within a frequency range of 100 to 1000 Hz [4]. In contrast, abnormal sounds come in various forms. Here, we will discuss two common types: Wheezes and Crackles.

**Wheezes** are long and musical sounds that last over 100 milliseconds. They occur during inhalation and exhalation, often caused by narrowed or restricted airways. Their frequency usually falls between 100 to 1000 Hz, but higher harmonics are also possible [4].

**Crackles**, conversely, are brief, non-musical sounds that signal sporadic airway openings, often due to secretions. We can further divide them into Fine and Coarse Crackles. Fine Crackles are short, with a frequency of around 650 Hz and a duration of about five milliseconds. Coarse Crackles last longer, over 15 milliseconds, and occur at lower frequencies, below 350 Hz [4].

Understanding these distinctions in pulmonary sounds is vital for developing automated systems for their detection. Electronic stethoscopes can convert lung sounds into digital signals, enabling the use of advanced anomaly detection algorithms in computer-aided medical diagnosis.

#### 2.1.1 Digital Representation of Sound

Sound signals, variations in air pressure known as sound waves, can be digitally represented in several ways. The following will give an overview of the used methods in this thesis.

**Waveforms** are the most straightforward representation, where the sound signal is a sequence of numbers  $x_n$  representing air pressure at time step  $n \in \mathbb{N}$ . The key parameter here is the sampling rate, which dictates how often the audio signal is sampled per second [2].

**Spectrogram** representations, unlike waveforms, allow for a visual examination of the sound signal. This involves transforming the signal from a real-valued time-domain to a complex-valued frequency-domain representation using the Discrete Fourier Transform (DFT), mathematically defined as

$$X_k = \sum_{n=0}^{N-1} x_n e^{-i2\pi \frac{k \times n}{N}}$$

. The result of this transformation provides a good overview of the frequencies that make up the sound signal. However, we are more interested in local events for non-stationary signals like respiratory sounds.

The Short Time Fourier Transform (STFT) helps obtain a representation that summarizes the sound signals' constituting frequencies while showing local changes in their distribution. It first divides the signal into short slices, also called windows. It then applies a windowing function to each slice, gradually reducing the signal amplitude towards the edges. This continuity between the windows is crucial for minimizing spectral leakage, a phenomenon where sudden changes in the signal between the windows get misinterpreted as sudden changes in the original signal. Finally, STFT involves applying a DFT on every window. We obtain a time-frequency representation typically visualized by converting  $X_k$  to the log-spectrum  $20\log_{10}||X_k||$  [2].

Mel-Spectrograms refine this representation by aligning frequencies to the mel scale, approximating human hearing perception. This transformation is mathematically expressed as  $m = 2595\log_{10}(1 + \frac{f}{700})$  as formulated by O'Shaughnessy (1987) [19].

**Mel-Frequency Cepstral Coefficients (MFCCs)** are used for dimensionality reduction in spectrograms to preserve essential information while reducing the number of coefficients. The process involves performing DFT on the waveform, computing the log amplitude spectrum, transforming the spectrum to the mel scale, and finally applying the Discrete Cosine Transform, a simplified version of the DFT resulting in a real-valued representation [2]. While not easily interpretable by humans, the resulting cepstrum is highly relevant for input into machine learning algorithms.

## 2.2 Fundamentals of Anomaly Detection

Anomaly detection is a process that identifies data points deviating from expected patterns, known as anomalies or outliers [6]. These deviations often signal critical changes in a system, requiring intervention. In healthcare, as discussed in section 2.1, anomalies in respiratory sound patterns can indicate various conditions.

Anomaly detection algorithms characterize normal behavior, flagging deviations as anomalies. However, the rarity of anomalies and the uncertainty in their distribution poses significant challenges. Because anomalies are much more infrequent by nature, datasets typically are heavily unbalanced and contain a much larger number of normal samples than anomalies. Furthermore, the anomalous data points can exhibit various forms of non-normality, meaning there can be a substantial variation within the set of outliers [21]. It is also essential to balance false positives and negatives based on the specific application domain.

Outlier detection can be categorized based on the data available:

1. **Supervised Anomaly Detection:** This method uses a fully labeled dataset to differentiate between normal and abnormal data points. However, the lack

of thorough datasets representing all the variance in anomalies limits these approaches.

2. **Unsupervised Anomaly Detection:** More common in real-world scenarios, this approach uses only normal data points, requiring the system to learn their defining characteristics autonomously.
3. **Weakly Supervised Anomaly Detection:** This approach, which we focus on in our research, uses primarily normal data points with a significantly smaller subset of anomalies. It is advantageous as it requires fewer anomalous data points than fully supervised methods while allowing for generalization abilities.

Anomaly detection algorithms may provide a direct classification of data points as normal or anomalous or output an anomaly score indicating deviation from normality. This score helps identify anomalous samples by finding a threshold above which all samples can be considered anomalous. Traditional methods like K-nearest neighbor (KNN) and Support Vector Machines (SVMs) rely on distance metrics or decision boundaries to identify outliers. KNN works by identifying data points significantly distant from the closest set, while SVMs create a boundary between classes, effective in scenarios with clear separation [6].

However, these traditional methods can be limited in handling complex, high-dimensional, and noisy data or when anomalies closely resemble normal data. Deep learning methods can extract features from raw data and have shown remarkable effectiveness in learning complex patterns, such as those in audio signals. We will explore two distinct deep-learning architecture families used in this research, highlighting their suitability for anomaly detection in respiratory sounds.

## 2.3 Reconstruction-Based Methods

Reconstruction-based methods in anomaly detection use reconstruction errors as anomaly scores to identify anomalies. These methods involve two primary steps: dimensionality reduction and data reconstruction. Initially, the data is transformed into a latent, more compact representation in a latent space. This space aims to retain essential data features while discarding noise and irrelevant details. The subsequent step involves reconstructing the original data from this compact representation. The core challenge lies in achieving a balance where the reduced representation is compact yet retains sufficient information for accurate reconstruction without overfitting.

These models are trained unsupervised, using only normal data points. This approach ensures that the model learns typical patterns of such. The reconstruction error is calculated during training, reflecting the accuracy with which the model can recreate the input data. The underlying assumption is that a model trained on normal data will yield minimal error in reconstructing similar data. However, when encountering anomalous data that deviates from learned patterns during evaluation or inference, the model faces difficulties in reconstruction, resulting in a higher reconstruction error. This error then serves as an anomaly score, with higher errors indicating a greater likelihood of anomaly and vice versa.



### 2.3.1 Essentials of Autoencoders

Autoencoders are a prevalent neural network architecture in reconstruction-based methods, known for their ability to learn compact data representations unsupervised. An autoencoder comprises two main components: the Encoder and the Decoder.

- **Encoder** ( $A : \mathbb{R}^n \rightarrow \mathbb{R}^l$ ): This component maps high-dimensional input data (dimensionality  $n$ ) into a lower-dimensional latent space (dimensionality  $l < n$ ). This process compresses the data into an efficient, compact form.
- **Decoder** ( $B : \mathbb{R}^l \rightarrow \mathbb{R}^n$ ): The Decoder performs the inverse function, reconstructing data from the latent space back to its original dimensionality. Its goal is to replicate the original input as closely as possible.

The optimization challenge in autoencoders can be formulated as follows:

$$\arg \min_{A,B} E[\Delta(\mathbf{x}, B \circ A(\mathbf{x}))],$$

where  $E$  represents the expected value of the reconstruction loss  $\Delta$  for input  $\mathbf{x}$  [3].

## 2.4 Density Estimation Methods

Density estimation methods in anomaly detection revolve around the concept of probability distributions. Probability distributions are mathematical functions that describe the probability associated with each possible value of a random variable. Suppose the random variable can take any value within a specific range. In that case, the probability distribution is continuous and can be described by a Probability Density Function (PDF), providing a probability of a random variable falling within a specific range.

For a continuous real-valued random variable  $X$ , the PDF is defined as

$$P(a \leq X \leq b) = \int_a^b f(x) dx$$

for all  $a, b \in \mathbb{R}$  [15]. Here,  $f(x)$  represents the probability density function of  $X$ . It is important to note that the PDF does not give probabilities directly. Instead, the area under the PDF curve between these points gives the probability of  $X$  falling within the interval from  $a$  to  $b$ .

Density estimation involves estimating the PDF from observed data by estimating a joint distribution  $p(\mathbf{x})$  from a set of examples  $\{\mathbf{x}^{(t)}\}_{t=1}^T$  [13]. The estimation can be parametric, where the data is assumed to follow a known distribution like Gaussian with the mean and standard deviation as parameters, or nonparametric, which does not presume a specific distribution and directly estimates the PDF from the data. Nonparametric methods can handle more complex distributions but usually require more data to produce an accurate estimate.

In anomaly detection, estimating the PDF of a dataset helps identify regions of low probability. Data points in these regions are potential anomalies, making density estimation a powerful tool for detecting outliers.

### 2.4.1 Introduction to Masked Autoencoders

Masked Autoencoders for Distribution Estimation (MADE) extend the concept of autoencoders so that they can understand the data distribution. Unlike tradi-

tional autoencoders, MADE enforces the autoregressive property and considers the input data order so that each output part is influenced only by preceding input parts.

The autoregressive property is accomplished by masking the weights in each autoencoder layer, controlling the information flow. Each neuron is labeled with a number from 1 to  $D - 1$  (where  $D$  is the input dimensionality) and the following rule is applied to determine allowed connections: a neuron in layer  $l$  (called  $k'$ ) can only be connected to a neuron in the previous layer  $l - 1$  (called  $k$ ) if its label is greater than or equal to the label of  $k$ . Mathematically, Germain et al. (2015) states this concept as

$$M_{k',k}^{w^l} = \begin{cases} 1, & \text{if } m^l(k') \geq m^{l-1}(k) \\ 0, & \text{otherwise.} \end{cases}$$

Here,  $M_{k',k}^{w^l}$  is the weight matrix mask that determines whether a connection is allowed or not. For the output layer, the rule needs the slight modification of making the condition strict ( $m^l(k') > m^{l-1}(k)$ ) to maintain the autoregressive property.

MADE's architecture allows for calculating the probability of observing the input  $\mathbf{x}$  as

$$p(\mathbf{x}) = \sum_{d=1}^D p(x_d | \mathbf{x}_{<d}).$$

This probabilistic model is beneficial in anomaly detection as it can identify data points with low probability, indicating potential anomalies.

## 2.5 Evaluation Metrics for Model Comparison

Evaluating and comparing the performance of different anomaly detection models requires carefully chosen metrics relevant to real-world applications and offers clear, intuitive interpretations of the models' effectiveness. Before introducing the five core metrics considered in this thesis, we need to understand the concept of a confusion matrix. In anomaly detection, we can categorize a model's prediction outcome into four types: true negatives (correct normal prediction), false negatives (anomalies incorrectly labeled as normal), true positives (correct anomaly prediction), and false positives (normal data points mistakenly identified as anomalies). A confusion matrix summarizes these four outcomes.

Having introduced the needed terminology, we focus on defining the evaluation metrics.

### Sensitivity (True Positive Rate - TPR)

$$\text{TPR} = \frac{\text{TruePositives}}{\text{TruePositives} + \text{FalseNegatives}}.$$

Sensitivity measures the proportion of actual anomalies correctly identified. It ranges from 0 (no anomaly detected) to 1 (perfect anomaly detection), with a higher value preferable, especially in critical applications like healthcare, where leaving an anomaly undetected can have serious implications.

**False Positive Rate (FPR)**

$$\text{FPR} = \frac{\text{FalsePositives}}{\text{TrueNegatives} + \text{FalsePositives}}.$$

FPR assesses the proportion at which normal data points are incorrectly classified as anomalies. It ranges from 0 (no false alarms) to 1 (all normal data classified as anomalies). A lower FPR is desired, as it indicates fewer false alarms.

**Specificity (True Negative Rate - TNR)**

$$\text{TNR} = \frac{\text{TrueNegatives}}{\text{TrueNegatives} + \text{FalsePositives}}.$$

Specificity quantifies how well the model identifies normal data points. It also ranges from 0 (poor recognition of normal conditions) to 1 (excellent recognition of normal conditions). Higher specificity is essential to minimize false alarms in sensitive domains like medical settings.

**Area Under the Curve (AUC)**

The Area Under the Curve (AUC) is a metric calculated using the Receiver Operating Characteristic (ROC) curve, which portrays the True Positive Rate (TPR) against the False Positive Rate (FPR) within a unit square, with TPR on the Y-axis and FPR on the X-axis. This visualization emphasizes the trade-off between a model's capability to correctly identify anomalies (TPR) and its tendency to misclassify normal data as anomalous (FPR).

In this graph, a point at (0,0) signifies a model that categorizes all data as normal, while (1,1) indicates a model labeling everything anomalous. The theoretical perfect model achieves flawless classification, represented by (0,1). The ROC curve emerges by systematically adjusting the model's classification threshold and plotting corresponding TPR and FPR values, forming a curve that illustrates performance across various thresholds [10].

A random model aligns with the diagonal line from (0,0) to (1,1) in binary classification tasks like anomaly detection. Performance surpasses randomness when the ROC curve lies above this diagonal and diminishes when below. The AUC is a quantitative measure of this performance, quantifying the area enclosed by the ROC curve and the x-axis. It ranges from 0.5 (no discrimination ability) to 1 (perfect classification). Notably, models with an AUC below 0.5 can be adjusted to achieve better-than-random classification.

A high AUC is crucial in medical diagnostics to detect pathologies while avoiding false alarms and overtreatment of healthy patients.

**Balanced Accuracy (BALACC)**

Balanced Accuracy (BALACC) assigns equal importance to correctly identifying anomalies and normal data points. It is calculated as the average of Sensitivity (True Positive Rate) and Specificity (True Negative Rate):

$$\text{BALACC} = 0.5 \times (\text{Sensitivity} + \text{Specificity})$$

This metric is especially useful in scenarios where the dataset is unbalanced, a common occurrence in anomaly detection where anomalies are much rarer

than normal samples. In such cases, traditional accuracy metrics can be misleading. For example, consider a dataset where 95% of the data points are normal and only 5% are anomalies. A model that naively classifies every data point as normal would achieve a 95% accuracy rate, which is misleadingly high. Balanced accuracy corrects this distortion by considering both the ability to detect anomalies (sensitivity) and recognize normal instances (specificity), providing a more truthful measure of a model's performance. In our example, it would only result in a 50% balanced accuracy.

Balanced accuracy has a goal similar to the AUC's: correctly identifying diseased and healthy individuals.

# Chapter 3

## Literature Review

### 3.1 Current State of Respiratory Sound Analysis

Lung auscultation is the standard method of diagnosing respiratory disease by listening to the patient's lungs through the chest. However, this approach, which relies on manual assessment by healthcare professionals, has several limitations. Its effectiveness depends on the physician's skill, experience and auditory sensitivity, leading to potential inaccuracies in diagnosis [20]. In addition, manual auscultation is typically limited to clinical settings, missing critical auditory cues that may occur outside of these settings, such as nocturnal breath sounds common in conditions such as asthma [22].

These limitations, combined with advances in technology, have led to the development of computerized respiratory sound analysis. In this approach, lung sounds are digitally recorded and then analyzed. Early techniques focused on the graphical representation of sound waves, allowing medical professionals to visually identify abnormalities. However, this method did not fully mitigate the risk of human error. Subsequently, statistical approaches were developed to assess the frequency of specific respiratory events based on historical data patterns. According to systematic reviews [20], machine learning based approaches provide the most promising results, but so far were limited by the lack of sufficiently large data sets.

#### 3.1.1 The ICBHI Challenge 2017

During the 2017 Annual International Conference on Biomedical and Health Informatics, a central challenge was launched in response to the scarcity of comprehensive lung sound data. This challenge aimed to foster the development and evaluation of advanced algorithms for automated lung sound classification, using a novel dataset curated specifically for this purpose. Known as the Respiratory Sound Database [23], this collection stands out as one of the earliest and most comprehensive publicly available datasets in the field, comprising 6898 respiratory cycles from 126 patients. These recordings, collected by professional teams in Greece and Portugal, represent a diverse range of audio samples, capturing sounds from healthy individuals as well as patients suffering from lung diseases such as COPD, asthma, and bronchiectasis. Each breathing cycle in the database is annotated by domain experts and categorized as normal, with wheezes, with crackles, or with both wheezes and crackles. The challenge encouraged a multitude of submissions, showcasing a range of innovative machine learning approaches. Below, we compare a selection of these methods.

### 3.1.2 Existing Approaches

Starting with traditional artificial intelligence methods, Jakovljević and Lončar-Turukalo (2018) published their work based on hidden Markov models (HMM) alongside the paper introducing the Respiratory Sound Database. [17]. Using MFCCs as features, they employed a four-class classifier with the official 60/40 split at the recording level, using 60% of the data for training and the remaining 40% for evaluation. The four classes were healthy, crackles, wheezes, both crackles and wheezes. A balanced accuracy score of 0.39 was achieved, with sensitivity of 0.38 and specificity of 0.41.

Chambres et al. (2018) used boosted decision trees (BDT) to address the four-class classification task [5]. They used the same 60/40 split and MFCCs as features. The model architecture significantly improved the balance accuracy to 0.49, with a sensitivity of 0.78 and a specificity of 0.21.

Shortly after, the use of neural networks gained traction. Ma et al. (2019) proposed the use of a bi-ResNet (LungBRN) architecture [24] consisting of multiple concatenated convolutional neural network layers [18]. Using the same split as the other approaches, but using short-time Fourier transform (STFT) and wavelet analysis to extract features, they achieved an official balanced accuracy of 0.5, specificity of 0.69, and sensitivity of 0.31 for the four-class problem.

The Microsoft Research India team around Gairola et al. (2021) published their RepireNet [12] network and benchmarked it in a variety of data splits and in a binary and four-class classification problem. The backbone are blocks of ResNet34 [16] deep convolutional neural networks (CNN). Using MelSpectrograms as features, their baseline CNN achieved 0.55 balanced accuracy on the official 60/40 split, 0.66 balanced accuracy for the four-class problem on a self-defined random 80/20 split at the breathing cycle level, and 0.72 on the same 80/20 split but treating the problem as a binary classification, which allows for an easier comparison to an anomaly detection setting.

Table 3.1: Performance comparisons of the showcased models

Model	Split	Features	Se	Sp	BALACC
HMM	60/40 4 class	MFCC	0.38	0.41	0.39
BDT	60/40 4 class	MFCC	0.78	0.21	0.49
LungBRN	60/40 4 class	STFT + Wavelet	0.69	0.31	0.5
RespireNet CNN	60/40 4 class	MelSpectrogram	0.39	0.71	0.55
RespireNet CNN	80/20 4 class	MelSpectrogram	0.54	0.79	0.66
RespireNet CNN	80/20 2 class	MelSpectrogram	0.61	0.83	0.72

It is important to note that all mentioned approaches to respiratory sounds analysis rely on treating it as a supervised classification task. These methods, while effective in their context, assume the availability of extensive labeled data representing various specific respiratory conditions. In real-world scenarios, however, such comprehensive data sets are not always readily available. Furthermore, the strict categorization of respiratory sounds into predefined classes may overlook the nuanced and unpredictable nature of respiratory anomalies. Therefore, the remainder of this thesis will explore respiratory sound analysis through the lens of anomaly detection.

## 3.2 Respiratory Sound Analysis from an Anomaly Detection Perspective

The use of anomaly detection methods to solve sound analysis problems is not a new concept. In particular, these methods have proven their effectiveness in the field of industrial sound analysis, as demonstrated in Task 2 of the annual DCASE Challenge [8], where machine condition monitoring is performed by observing the sound produced by these machines. The sound emitted can be either normal or anomalous, and machine learning algorithms learn to understand the characteristics of healthy machine sounds in order to accurately predict machine failure in the case of anomalous sounds such as rattling or whirring.

A similar approach can be used in breathing sound analysis. The different anomalous respiratory sounds can all be grouped into a single anomaly class, and anomaly detection models can learn the constitution of healthy respiratory cycles. If a sample deviates significantly from the learned representation of a healthy sound, the system can flag it as anomalous.

## 3.3 Variational Autoencoders

Cozzatti et al. (2022) [7] explored the first anomaly detection approach to the respiratory sound database. In their work, MFCCs were used as features and the breathing cycles containing wheezes, crackles or both were all summarized in an anomaly class. A Variational Autoencoder (VAE) was trained using only known healthy breathing cycles.

Variational Autoencoders are similar to Autoencoders in that they consist of an encoder and a decoder part. The encoder of a VAE, by comparison, uses variational inference to output the parameters of a continuous and easily sampled distribution, usually the mean and standard deviation of a Gaussian [7]. As a result, the input to the decoder is a single sample from that predicted distribution. This allows the model to provide a measure of certainty of the reconstructed data using the variability of the latent space [1].

By training the VAE with normal sounds only, it learns to accurately reconstruct physiological respiratory cycles. The reconstruction error reported by the model is small in this case. When the model attempts to reconstruct a respiratory sound with pathologies, the parameters of the Gaussian will most likely not match the parameters of the learned distribution of healthy sounds, and thus the reconstruction will have a higher error. The paper then used a small subset of the original dataset, containing both healthy and unhealthy lung sounds, to determine a threshold in the reconstruction error above which all higher errors should be marked as anomalous, making the process weakly supervised. The proposed model achieved competitive results in the binary class problem, with a balanced accuracy of 0.57 for the official 60/40 split and 0.6 for a random 80/20 split.

## 3.4 Group Masked Autoencoders

In section 2.4.1, we have discussed how Masked Autoencoders are an alternative anomaly detection approach to generative models by evaluating probability densities. The basic concept focused on modifying an existing autoencoder

Table 3.2: Performance of the proposed method

Split	Se	Sp	BALACC
60/40	0.33	0.80	0.57
80/20	0.58	0.61	0.60

structure to satisfy the autoregressive property by masking the weights of the neural network layers so that each output dimension depends only on the preceding input dimensions.

When dealing with representations of sound data, such as MelSpectrograms or MFCCS, the interest shifts from the autoregressive ordering of individual input dimensions to the ordering of sound frames. Here, Group Masked Autoencoders (GMADE) [14] provide a more tailored approach for audio anomaly detection tasks where temporal context is important. GMADE differs from traditional MADE in that it does not split the joint distribution into individual dimensional conditions, but rather over grouped frames. This approach is particularly relevant when dealing with sound data, where each time frame in a MelSpectrogram is considered a separate group.

In GMADE, the input space has the dimensionality  $T \times M$ , where  $T$  is the number of frames concatenated in the input and  $M$  is the number of Mel frequency bands. If an input sample can be thought of as  $\mathbf{t} = [\mathbf{t}_{i+1}, \mathbf{t}_{i+2}, \dots, \mathbf{t}_{i+T}]$  with  $\mathbf{t}_i \in \mathbb{R}^{M \times 1}$ , the joint density can be decomposed as

$$p(\mathbf{t}) = \sum_{i=1}^T p(\mathbf{t}_i | \mathbf{t}_{<i})$$

where the probability of each frame depends on all previous frames and their mel bins and no other frames [14]. To maintain the autoregressive property, the generation of the weight matrices must be slightly adapted from the MADE approach to assign labels to the neurons only from 1 to  $T - 1$  to correctly zero connections between groups instead of units.

The paper also explored orderings other than causal, where a frame can only depend on its predecessors. Backward ordering predicts the probability density of frames given only their succeeding frames, while middle frame ordering attempts to predict the middle frame given only the frames surrounding it. Ensembles of all three approaches were also evaluated. GMADE achieved state of the art results in Task 2 of the DCASE Challenge 2020 in the machine condition monitoring task, especially for non-stationary sounds. While this is promising for respiratory sound analysis due to the non-stationary nature of lung sounds, the efficacy of GMADE in detecting anomalies in respiratory sounds is yet to be tested.



# **Chapter 4**

## **Methodology**

### **4.1 Dataset**

#### **4.1.1 Definition**

#### **4.1.2 Data Splitting**

### **4.2 Preprocessing**

### **4.3 Detailed Overview of the Models**

#### **4.3.1 Implementation of the VAE**

#### **4.3.2 Implementation of the G-MADE**

# **Chapter 5**

## **Experiments and Results**

### **5.1 Experimental Setup**

### **5.2 Generalization Capabilities**

### **5.3 Age and Gender Differences in Model Accuracy**

### **5.4 Model Sensitivity to Noise**

### **5.5 Model Performance on Crackles and Wheezes**

### **5.6 Impact of Hyperparameter Variations**

### **5.7 Assessment of Data Splitting at Recording Level**

### **5.8 Comparison of Feature Extraction Methods: MFCC vs. MelSpectrogram**

### **5.9 Interpretability and Explainability of the Proposed Models**

### **5.10 Comparative Analysis and Discussion**

# **Chapter 6**

## **Conclusion and Outlook**

### **6.1 Summary of Findings**

### **6.2 Potential Applications and Practical Implications**

### **6.3 Limitations of the Proposed Approaches**

### **6.4 Directions for Future Research**

# Bibliography

- [1] Jinwon An and Sungzoon Cho. 2015. Variational autoencoder based anomaly detection using reconstruction probability. *Special lecture on IE*, 2, 1, 1–18.
- [2] Tom Bäckström, Okko Räsänen, Abraham Zewoudie, Pablo Perez Zarazaga, Sneha Das, et al. 2020. Introduction to speech processing. (2020).
- [3] Dor Bank, Noam Koenigstein, and Raja Giryes. 2023. Autoencoders. *Machine Learning for Data Science Handbook: Data Mining and Knowledge Discovery Handbook*, 353–374.
- [4] Abraham Bohadana, Gabriel Izbicki, and Steve S Kraman. 2014. Fundamentals of lung auscultation. *New England Journal of Medicine*, 370, 8, 744–751.
- [5] Gaëtan Chambres, Pierre Hanna, and Myriam Desainte-Catherine. 2018. Automatic detection of patient with respiratory diseases using lung sound analysis. In *2018 International Conference on Content-Based Multimedia Indexing (CBMI)*. IEEE, pp. 1–6.
- [6] Varun Chandola, Arindam Banerjee, and Vipin Kumar. 2009. Anomaly detection: A survey. *ACM computing surveys (CSUR)*, 41, 3, 1–58.
- [7] Michele Cozzatti, Federico Simonetta, and Stavros Ntalampiras. 2022. Variational autoencoders for anomaly detection in respiratory sounds. In *International Conference on Artificial Neural Networks*. Springer, pp. 333–345.
- [8] DCASE. 2023. DCASE2023 Challenge - DCASE — dcase.community. <https://dcase.community/challenge2023/index>. [Accessed 30-11-2023]. (2023).
- [9] J Earis. 1992. Lung sounds. *Thorax*, 47, 9, 671.
- [10] Tom Fawcett. 2006. An introduction to ROC analysis. *Pattern recognition letters*, 27, 8, 861–874.
- [11] Thomas Ferkol and Dean Schraufnagel. 2014. The global burden of respiratory disease. *Annals of the American Thoracic Society*, 11, 3, 404–406.
- [12] Siddhartha Gairola, Francis Tom, Nipun Kwatra, and Mohit Jain. 2021. Respirenet: A deep neural network for accurately detecting abnormal lung sounds in limited data setting. In *2021 43rd Annual International Conference of the IEEE Engineering in Medicine & Biology Society (EMBC)*. IEEE, pp. 527–530.
- [13] Mathieu Germain, Karol Gregor, Iain Murray, and Hugo Larochelle. 2015. Made: Masked autoencoder for distribution estimation. In *International conference on machine learning*. PMLR, pp. 881–889.
- [14] Ritwik Giri, Fangzhou Cheng, Karim Helwani, Srikanth V. Tenneti, Umut Isik, and Arvindh Krishnaswamy. 2020. Group masked autoencoder based density estimator for audio anomaly detection. In *Detection and Classification of Acoustic Scenes and Events Workshop 2020*. <https://www.amazon.science/publications/group-masked-autoencoder-based-density-estimator-for-audio-anomaly-detection>.

- [15] Charles Miller Grinstead and James Laurie Snell. 2006. *Grinstead and Snell's introduction to probability*. Chance Project.
- [16] Kaiming He, Xiangyu Zhang, Shaoqing Ren, and Jian Sun. 2016. Deep residual learning for image recognition. In *Proceedings of the IEEE conference on computer vision and pattern recognition*, pp. 770–778.
- [17] Nikša Jakovljević and Tatjana Lončar-Turukalo. 2018. Hidden markov model based respiratory sound classification. In *Precision Medicine Powered by pHealth and Connected Health: ICBHI 2017, Thessaloniki, Greece, 18–21 November 2017*. Springer, pp. 39–43.
- [18] Yi Ma, Xinzi Xu, Qing Yu, Yuhang Zhang, Yongfu Li, Jian Zhao, and Guoxing Wang. 2019. Lungbrn: A smart digital stethoscope for detecting respiratory disease using bi-resnet deep learning algorithm. In *2019 IEEE Biomedical Circuits and Systems Conference (BioCAS)*. IEEE, pp. 1–4.
- [19] Douglas O'shaughnessy. 1987. *Speech communications: Human and machine (IEEE)*. Universities press.
- [20] Rajkumar Palaniappan, Kenneth Sundaraj, Nizam Uddin Ahamed, Agilan Arjunan, and Sebastian Sundaraj. 2013. Computer-based respiratory sound analysis: a systematic review. *IETE Technical Review*, 30, 3, 248–256.
- [21] Guansong Pang, Chunhua Shen, Longbing Cao, and Anton Van Den Hengel. 2021. Deep learning for anomaly detection: A review. *ACM computing surveys (CSUR)*, 54, 2, 1–38.
- [22] Renard Xaviero Adhi Pramono, Stuart Bowyer, and Esther Rodriguez-Villegas. 2017. Automatic adventitious respiratory sound analysis: A systematic review. *PloS one*, 12, 5, e0177926.
- [23] BM Rocha, Dimitris Filos, L Mendes, Ioannis Vogiatzis, Eleni Perantoni, Evangelos Kaimakamis, P Natsiavas, Ana Oliveira, C Jácome, A Marques, et al. 2018. A respiratory sound database for the development of automated classification. In *Precision Medicine Powered by pHealth and Connected Health: ICBHI 2017, Thessaloniki, Greece, 18–21 November 2017*. Springer, pp. 33–37.
- [24] Runze Wang, Yanan Guo, Wendao Wang, and Yide Ma. 2019. Bi-ResNet: fully automated classification of unregistered contralateral mammograms. In *Artificial Neural Networks and Machine Learning–ICANN 2019: Workshop and Special Sessions: 28th International Conference on Artificial Neural Networks, Munich, Germany, September 17–19, 2019, Proceedings 28*. Springer, pp. 273–283.